

# Tuning of Silver Cluster Emission from Blue to Red Using a Bio-Active Peptide in Water

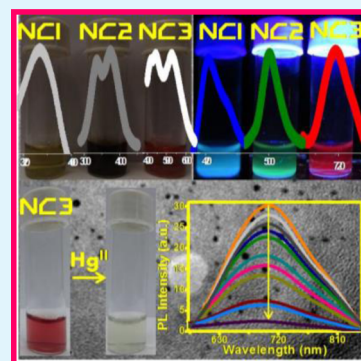
Subhasish Roy, Abhishek Baral, and Arindam Banerjee\*

Department of Biological Chemistry, Indian Association for the Cultivation of Science, Jadavpur, Kolkata 700032, India

## S Supporting Information

**ABSTRACT:** Blue, green, and red emitting silver quantum clusters have been prepared through green chemical approach by using a bio-active peptide glutathione (reduced) in a 50 mM phosphate buffer at pH 7.46. This study describes fluorescence emission tuning of the silver clusters by making different sized Ag clusters using slightly different reaction conditions keeping the same stabilizing ligand, reducing agent, solvent system, and silver salt precursor. The preparation procedure of these silver quantum clusters is new and highly reproducible. Each of these clusters shows very interesting fluorescence properties with large Stokes shifts, and the quantum yields of blue, green, and red clusters are 2.08%, 0.125%, and 1.39%, respectively. These silver quantum clusters have been characterized by using different techniques including fluorescence spectroscopy, UV-vis spectroscopy, field-emission gun transmission electron microscopic (FEG-TEM) imaging and MALDI-TOF MS analyses. MALDI-TOF MS analyses show that the size of these blue, green and red emitting silver clusters are Ag<sub>5</sub> (NC1, nanoclusters 1), Ag<sub>8</sub> (NC2, nanoclusters 2) and Ag<sub>13</sub> (NC3, nanoclusters 3), respectively, by using 2,5-dihydroxybenzoic acid as a matrix. These clusters are stable in broad ranges of pH. The NC3 (red emitting) has been successfully utilized for selective and sensitive detection of toxic Hg<sup>II</sup> ions in water by using even naked eyes, fluorometric, and calorimetric studies. The lower limit of detection of Hg<sup>II</sup> ions in water has been estimated to be 126 and 245 nM from fluorometric and UV-vis analyses, respectively. Enthalpy change ( $\Delta H$ ) during this Hg<sup>II</sup> sensing process is 2508 KJ mol<sup>-1</sup>.

**KEYWORDS:** Peptide, silver cluster, physiological pH, tuning of fluorescence emission, mercury(II) sensing, naked eye detection



## INTRODUCTION

Conventional fluorophores such as organic dyes and semi-conducting quantum dots have their limitations due to poor photostability, toxicity, and poor biological applicability. However, noble metal clusters<sup>1–7</sup> are very promising alternatives for sensing,<sup>8–15</sup> imaging,<sup>16–23</sup> and other applications<sup>24–29</sup> owing to their tiny size, excellent photostability against photobleaching, good processability, and extremely low toxicity. Noble metal nanoparticles show surface plasmon resonance and size dependent optical property.<sup>30</sup> Further reduction of size of gold and silver nanoparticles down to 2 nm or below creates a fascinating fluorescence property of these elements in their respective tiny form.<sup>1–7</sup> These clusters exhibit a molecule-like electronic transition. Generally, the synthesis of silver quantum clusters involves first the reduction of Ag<sup>I</sup> salts to Ag<sup>0</sup> and then subsequent stabilization of these nascent clusters by using suitable stabilizing agents. There are different techniques for the reduction including radiolytical,<sup>31</sup> photochemical,<sup>32</sup> sonochemical,<sup>33</sup> electrochemical,<sup>34</sup> and chemical<sup>35</sup> methods. Various stabilizing agents including dendrimers,<sup>32</sup> proteins,<sup>36</sup> thiols,<sup>37</sup> peptides,<sup>38</sup> and others<sup>39–41</sup> have been utilized. Though there are many reports on organic phase synthesis of silver quantum clusters,<sup>34</sup> preparation and stabilization of silver quantum clusters in aqueous medium is still challenging and water dispersible fluorescent quantum clusters have immense applications in biochemical sensing and

bio-imaging.<sup>1</sup> Peptides with free thiol, carboxylic acid, and amino group are good stabilizing agents for silver/gold quantum clusters due to their good water solubility and thermodynamic stability. Though there are several methods of preparing and stabilizing gold and silver quantum clusters, there exists only a few reports to tune the fluorescence emission of gold or silver clusters by making different sized gold/silver quantum clusters. Synthesis of Ag<sub>15</sub> clusters using bovine serum albumin (BSA) by a simple wet chemical route has been reported.<sup>35</sup> Mercaptosuccinic acid has been utilized for the synthesis of Ag<sub>7</sub> cluster using sodium borohydride as a reducing agent.<sup>39</sup> Mattoussi and co-workers have developed polyethylene glycol appended lipoic acids for the synthesis of highly fluorescent silver quantum clusters.<sup>41</sup> Jin and co-workers have reported the synthesis of silver quantum clusters using *meso*-2,3-dimercaptosuccinic acid as a stabilizing agent and sodium borohydride as a reducing agent.<sup>37</sup> Zhu and co-workers have reported the intracellular imaging and nuclear staining by using silver quantum clusters.<sup>17</sup> Pradeep and co-workers have demonstrated the catalytic property of metal oxide supported silver quantum clusters for the reduction of various nitro compounds.<sup>42</sup> There are a few reports on the variation of the

Received: December 4, 2013

Accepted: February 25, 2014

Published: February 25, 2014

gold/silver cluster size either by changing the solvent or by the alteration of stabilizing ligand.<sup>38,43–46</sup> However, preparation of different sized silver quantum clusters with different color fluorescence emission using the same solvent, silver salt precursor, stabilizing ligand and reducing agent is really a challenging issue. So, there is a real need for the research and development of making different sized silver clusters with tunable emissive property from blue to red in water at physiological pH by using the same silver salt, reducing agent, stabilizing ligand and the solvent system.

In this study, we report the synthesis and characterization of three distinct colors: blue (NC1: nanocluster 1), green (NC2: nanocluster 2), and red (NC3: nanocluster 3) emitting fluorescent silver quantum clusters by using sodium borohydride (reducing agent), a bio-active peptide, reduced form of glutathione (stabilizing ligand) and silver salt ( $\text{AgNO}_3$ ) in water at pH 7.46. Interestingly, the preparation of blue and green emitting silver clusters shared similar reaction conditions including the same amount of ligand, same amount of reducing agent, solvent, and temperature used, except the different concentration of the silver salt used. The condition for making a red emitting silver cluster is different from those of blue and green emitting silver clusters, as relatively low temperature is used for making the red emitter Ag cluster, keeping other conditions including solvent system, the stabilizing ligand, reducing agent, and precursor silver salt identical. MALDI-TOF MS analysis clearly reveals that these three different color emitting clusters have different sizes:  $\text{Ag}_5$  is blue emitting,  $\text{Ag}_8$  is green emitting and  $\text{Ag}_{13}$  is red emitting. Moreover, the red emitting silver quantum clusters have shown very selective and highly sensitive detection of highly toxic  $\text{Hg}^{\text{II}}$  ions in water not only by using fluorescence spectroscopic method but also through naked eyes.

## EXPERIMENTAL SECTION

**Materials.** Reduced glutathione and sodium borohydride were purchased from local chemicals SRL, India. Other chemicals including  $\text{AgNO}_3$ ,  $\text{Na}_2\text{HPO}_4$ , and  $\text{NaH}_2\text{PO}_4$  were purchased from Merck, Germany. Reference dyes for quantum yield calculation were purchased from Sigma-Aldrich, USA. Water used for this study was ultra pure Milli-Q grade.

**Synthesis of Blue Emitting Silver Quantum Cluster (NC1).** 10 mg of reduced glutathione was taken in a 50 mL round bottom flask. 4 mL of 50 mM phosphate buffer of pH 7.46 was added to it. 1 mg of  $\text{AgNO}_3$  in 500  $\mu\text{L}$  Milli-Q water was added to that solution and stirred for a few minutes at room temperature. The round bottom flask was then fitted with a bulb condenser and the reaction environment was made inert by using argon gas balloon fitted to the condenser. The total set up was put into an oil bath and it was kept under vigorous stirring with a bath temperature of 140  $^\circ\text{C}$ . Two milligrams of  $\text{NaBH}_4$  in 500  $\mu\text{L}$  of Milli-Q water was then added to the hot reaction mixture slowly. The progress of the reaction was monitored using fluorescence spectroscopic and UV–vis studies. After 16 h of reaction time, the total solution became very light brown in color. This solution showed a blue color luminescence behavior under an UV torch of wavelength 365 nm. This NC1 solution was used for all studies without any purification.

**Synthesis of Green Emitting Silver Quantum Cluster (NC2).** The synthetic procedure for the preparation of the green emitting silver quantum cluster (NC2) was somewhat similar to that of NC1, except the amount of  $\text{AgNO}_3$  used was 5 mg in 500  $\mu\text{L}$  of Milli-Q water. This as-prepared solution showed a green color luminescence behavior under an UV torch of wavelength 365 nm. This NC2 solution was used for all studies without any purification.

**Synthesis of Red Emitting Silver Quantum Cluster (NC3).** Here 5 mg of reduced glutathione was taken in a 5 mL glass vial. 1.8

mL of 50 mM phosphate buffer of pH 7.46 was added to it. Then 1 mg of  $\text{AgNO}_3$  was added to that solution and stirred for a few minutes at ice cold condition. Next, 2 mg of  $\text{NaBH}_4$  was dissolved in 1 mL of cold Milli-Q water and 200  $\mu\text{L}$  of cold borohydride solution was added to the ice-cold solution mixture slowly. The progress of reaction was monitored using fluorescence spectroscopic and UV–vis studies. After 30–40 min of reaction time, the total solution became reddish in color. This solution showed a red color luminescence behavior under an UV torch of wavelength 365 nm. This NC3 solution was used for all studies without any purification.

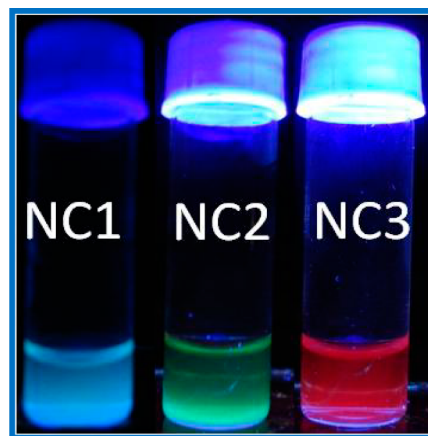
These procedures for the preparation of silver quantum clusters are totally new in phosphate buffer of pH 7.46 in water. This procedure helps to create blue, green, and red emitting silver quantum clusters with high quantum yields.

## RESULTS AND DISCUSSION

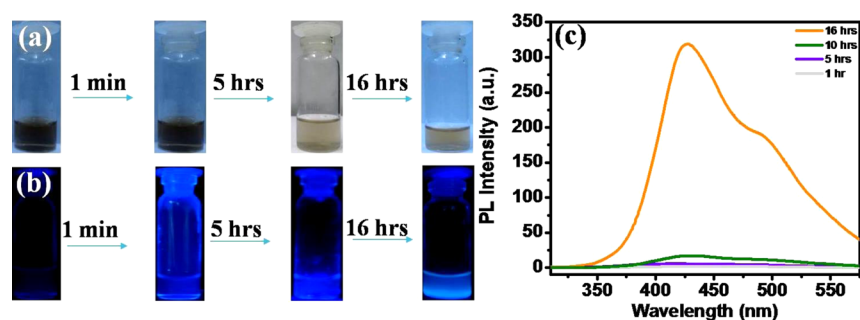
Mukherjee and co-workers have reported syntheses of two different,  $\text{Ag}_9$  and  $\text{Ag}_{14}$ , silver quantum clusters stabilized by a circulatory protein, human serum albumin (HSA).<sup>7</sup> However, we report three different,  $\text{Ag}_5$ ,  $\text{Ag}_8$ , and  $\text{Ag}_{13}$ , silver quantum clusters using a bio-active peptide glutathione (in its reduced form) at physiological pH using the same reducing agent, same stabilizing ligand and same solvent system. Moreover, the red emitting silver quantum cluster,  $\text{Ag}_{13}$ , has been utilized for the selective and sensitive detection of  $\text{Hg}^{\text{II}}$  ions in water.

**Size-Tuning of Silver Quantum Clusters.** The aim of this work is to tune the size of silver quantum clusters by using the same solvent, same silver salt precursor, same stabilizing ligand, and same reducing agent. In this study, different synthetic techniques (by varying temperature and the concentration of silver salt precursor) were exploited to synthesize silver quantum clusters with a wide variation in size. All three clusters, NC1, NC2, and NC3, were prepared in phosphate buffer at pH 7.46. However, the ratio of silver salt and temperature were varied widely. Hot reaction conditions were employed to prepare NC1 and NC2, but the ice-cold condition was necessary for the synthesis of NC3 to achieve our target of different-sized silver clusters. As a consequence, different quantum clusters exhibit different fluorescence color emission namely blue, green and red for NC1, NC2, and NC3, respectively. Detailed study of these clusters is mentioned in the succeeding section.

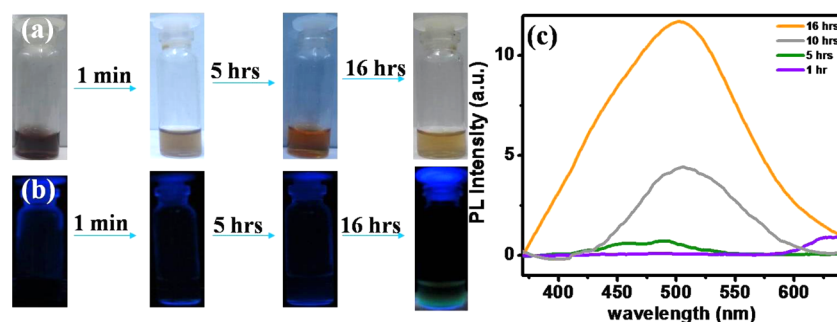
**UV–Vis Study.** Figure 1 shows photographs of various light emitting (blue, green, and red) silver clusters upon the irradiation of corresponding clusters at 365 nm wavelength.



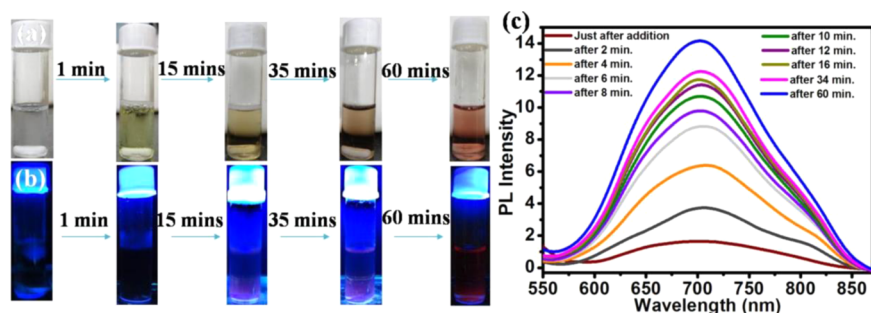
**Figure 1.** Emissive nature of the silver quantum clusters in presence of UV light at irradiation at 365 nm.



**Figure 2.** Time dependent color changes and formation of NC1 silver quantum cluster (a) under visible light, (b) under UV light, and (c) fluorescence spectroscopic emission profiles of the formation kinetics of NC1.



**Figure 3.** Time dependent color changes and formation of NC2 silver quantum cluster (a) under visible light, (b) under UV light, and (c) fluorescence spectroscopic emission profiles of the formation kinetics of NC2.



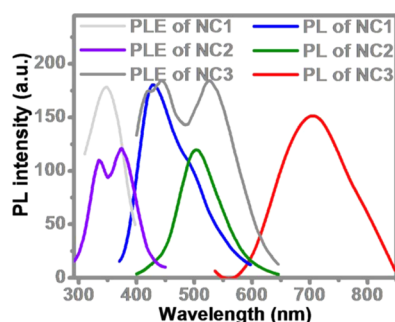
**Figure 4.** Time dependent color changes and formation of NC3 silver quantum cluster (a) under visible light, (b) under UV light and (c) fluorescence spectroscopic emission profiles of the formation kinetics of the red emitting cluster NC3.

Figure S1 (Supporting Information) reveals UV–vis absorption spectra of the corresponding silver clusters. Kinetics of the formation of blue (NC1) and green (NC2) emitting silver quantum clusters are shown in Figures S2 and S3 (Supporting Information), respectively. No significant absorption band in the visible region corresponding to the blue emitting (NC1) silver cluster is observed from the Figure S2 (Supporting Information) and this is supported by previous experimental results by other groups.<sup>46</sup> Figures 2a, 3a, and 4a show photographs of the kinetics of formation of NC1, NC2, and NC3, respectively, taken at different time intervals. No significant absorption band in UV–vis for NC2 was also observed initially. However, a small absorption peak was found at 300 nm after the completion of green emitting (NC2) cluster formation (Figure S3, Supporting Information). This suggests that the cluster size is small for either blue or green emitting clusters consisting of only a few atoms of silver.<sup>47</sup> However, initially, two absorption bands were observed during the process of synthesis of red emitting (NC3) quantum cluster at 485 and 530 nm (Figure S4, Supporting Information) and the

intensity of the 530 nm absorption peak was increased gradually with respect to time. The presence of an absorption band in the visible region clearly suggests the presence of several silver atoms within the cluster and the cluster size is bigger than the blue or green emitting cluster.<sup>48</sup> Time dependent color changes and formation of NC1, NC2, and NC3 clusters under visible light as well as under UV light are shown in Figures 2a,b, 3a,b, and 4a,b, indicating intense blue, green, and red color emissions, respectively.

**Fluorescence Study.** All three clusters emit different colors as it is evident from respective fluorescence studies. Figures 2c, 3c, and 4c show time dependent formation of all these clusters NC1, NC2, and NC3, respectively. It takes some time to exhibit fluorescence emission for all three clusters and after the completion of the formation, the fluorescence intensity reaches its maximum value. Photoluminescence emission (PL) and photoluminescence excitation (PLE) spectra of these clusters are shown in Figure 5. The blue emitting cluster (NC1) shows a fluorescence emission peak at 430 nm with a small hump at 500 nm and the corresponding PLE is observed at 347 nm. The





**Figure 5.** Photoluminescence emission (PL) and photoluminescence excitation (PLE) spectra of three different Ag clusters NC1, NC2, and NC3. The emission of each cluster is indicated by the corresponding color.

green emitting cluster NC2 shows a fluorescence emission peak at 505 nm and PLE is observed at 373 and 335 nm, whereas the red emitting cluster shows a fluorescence emission peak at 700 nm with a PLE at 442 and 527 nm. Emission profiles of these clusters with different excitation wavelengths are shown in Figure S5, S6, and S7 (Supporting Information) for NC1, NC2, and NC3, respectively, to examine whether these emissions are real or not. The position of fluorescence emission peak has not been changed with different excitation wavelengths suggesting the fluorescence emissions are real in nature.

Fluorescence quantum yield of these clusters have been estimated to be 2.08% for NC1 with the help of reference dye quinine sulphate, 0.125% for NC2 with respect to quinine sulphate, and 1.39% for NC3 with the help of reference dye atto 520. Estimated quantum yields (for NC1 and NC3) are almost comparable with the previously reported quantum yield for a red emitting silver quantum cluster stabilized by glutathione.<sup>49</sup> This quantum yield is also comparable to our previously reported quantum yield for silver quantum cluster stabilized by a gelator peptide inside the gel matrix.<sup>50</sup> Fluorescence excited state average life times of these clusters have been estimated by using excited-emission wavelengths at 340–430, 370–500, and 440–700 nm for NC1, NC2, and NC3 silver clusters, respectively. Fluorescence excited state average life times of these clusters have been estimated to be 1.31 ns for NC1, 5.55 ns for NC2, and 0.5 ns for NC3. Decay profiles of these clusters are shown in the Figure 6. pH stability

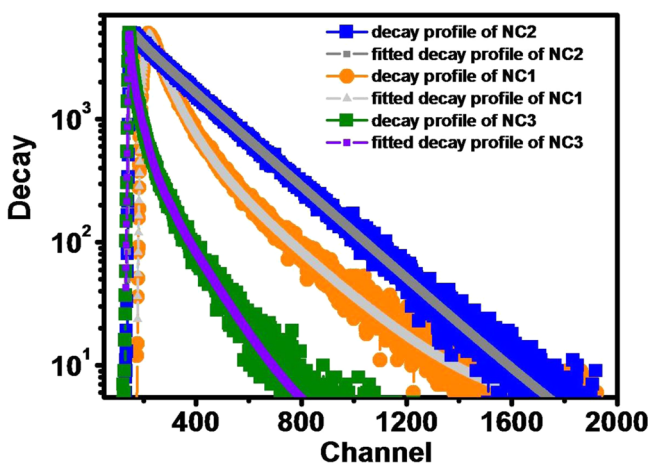


**Figure 6.** Fluorescence decay profile of the NC3 (average life time: NC1 = 1.31 ns, NC2 = 5.55 ns, and NC3 = 0.5 ns).

of these three clusters was also checked by using fluorescence spectroscopy. The blue emitting cluster (NC1) is stable from pH 5.60 to pH 11.00 (Figure S8, Supporting Information), whereas the green emitting cluster (NC2) is very stable at pH 5.60 to pH 13.20 (Figure S9, Supporting Information) and the red emitting cluster (NC3) is stable between pH 5.60 to pH 11.00 (Figure S10, Supporting Information). All clusters are stable at physiological pH 7.46 and they exhibit extreme stability at pH 5.60.

**Transmission Electron Microscopic Study.** Transmission electron microscopic study of these as-synthesized clusters reveals that the majority of these particles are  $\leq 2$  nm in size (Figure 7a,c,e). Figure 7b,d,f shows the particle size distribution

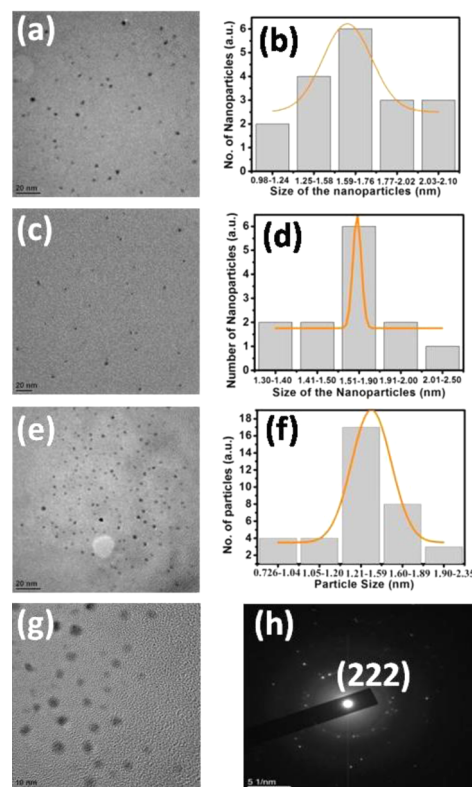


**Figure 7.** TEM images of (a) NC1, (c) NC2, and (e) NC3, particle size distribution diagram of (b) NC1, (d) NC2, and (f) NC3 obtained from their corresponding TEM images, (g) HR-TEM image of the NC3 (enlarged view showing the lattice fringe) and (h) the selected area electron diffraction analysis of the red emitting cluster NC3 suggesting the (222) lattice plane responsible for silver quantum cluster formation.

of the corresponding blue, green, and red emitting clusters. The HR-TEM image and the corresponding electron diffraction analysis of NC3 are shown in Figure 7g,h, respectively. All these clusters exhibit a narrow size distribution pattern, as it is evident from Figure 7b,d,f.

**FT-IR Study.** FT-IR spectral analyses were performed to get insight about the linkage pattern of the Ag atoms with the stabilizing ligand (reduced glutathione). The ligand shows a peak at  $2526\text{ cm}^{-1}$  corresponding to the  $-\text{SH}$  group (Figure S11, Supporting Information). After the formation of the silver cluster, no peak was observed at  $2526\text{ cm}^{-1}$ . This clearly suggests the involvement of the  $-\text{SH}$  group in the stabilization of silver quantum clusters.

**MALDI-TOF MS Analysis.** The exact size of these silver quantum clusters were determined by using MALDI-TOF MS analyses. Number of silver atoms present within the clusters was determined by using 2, 5-dihydroxy benzoic acid as a matrix in MALDI-TOF MS analyses (Figure 8). The NC1

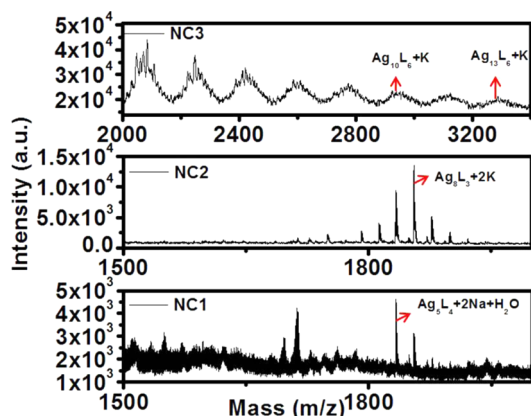


**Figure 8.** MALDI TOF MS analyses of three (NC1, NC2 and NC3) clusters in 2,5-dihydroxy benzoic acid.

(blue emitting) is composed of five atoms, NC2 (green emitting) is composed of 8 atoms and NC3 (red emitting) is composed of 13 atoms of silver along with some ligands. According to MALDI-TOF MS analysis the presence of peak for NC1 at  $m/z$  1833 is corresponding to the  $[\text{Ag}_5\text{L}_4 + 2\text{Na} + \text{H}_2\text{O}]^+$ , the peak for NC2 at 1856 is corresponding to the  $[\text{Ag}_8\text{L}_3 + 4\text{H}_2\text{O}]^+$ , and another peak for NC3 at 3285 is corresponding to the  $[\text{Ag}_{13}\text{L}_6 + \text{K}]^+$  along with another identified fragmented peak at  $m/z$  2961 corresponding to the  $[\text{Ag}_{10}\text{L}_6 + \text{K}]^+$ . This is the first report of synthesis of  $\text{Ag}_5$ ,  $\text{Ag}_8$ , and  $\text{Ag}_{13}$  clusters using the same ligand, same reducing agent, same silver salt precursor and same solvent system to the best of our knowledge.

**Metal Ion Sensing.** It is interesting to note that the red emitting silver quantum cluster NC3 has been nicely utilized for selective and sensitive detection of toxic  $\text{Hg}^{\text{II}}$  in water by using fluorescence spectroscopy, UV–vis spectroscopy, and isothermal titration calorimetry. The as-synthesized silver cluster NC3 is reddish pink in color and after the addition of  $\text{Hg}^{\text{II}}$  ions it becomes colorless and it is observed also through naked eyes (Figure S12, Supporting Information). Similarly, the fluorescence intensity of this as-prepared red emitting silver cluster is decreased gradually by the gradual addition of  $\text{Hg}^{\text{II}}$  ions in water. The minimum detectable limit of fluorescence quenching is estimated to be 126 nM  $\text{Hg}^{\text{II}}$  ions and the addition of 6.11  $\mu\text{M}$  of  $\text{Hg}^{\text{II}}$  ions causes almost complete quenching of fluorescence intensity of the silver cluster (Figure 9). It is interesting also to examine the selectivity of aqueous  $\text{Hg}^{\text{II}}$  ions detection in the presence of other metal ions including  $\text{Zn}^{\text{II}}$ ,  $\text{Cd}^{\text{II}}$ ,  $\text{Fe}^{\text{II}}$ ,  $\text{Ca}^{\text{II}}$ ,  $\text{Mg}^{\text{II}}$ ,  $\text{Mn}^{\text{II}}$ ,  $\text{Cu}^{\text{II}}$ ,  $\text{Sr}^{\text{II}}$ ,  $\text{Al}^{\text{III}}$ ,  $\text{Ni}^{\text{II}}$ ,  $\text{Co}^{\text{II}}$ ,  $\text{Pt}^{\text{II}}$ , and  $\text{Pb}^{\text{II}}$ , as it is evident from Figure S13 (Supporting Information).  $\text{Cu}^{\text{II}}$  and  $\text{Pb}^{\text{II}}$  show very small quenching of the fluorescence intensity compared to that of  $\text{Hg}^{\text{II}}$  ions (Figure S13, Supporting Information). However, other metal ions are totally silent toward the fluorescence quenching of the NC3 quantum cluster. Relative fluorescence intensity of the silver quantum cluster is plotted toward the effect of other metal ions and it is shown in Figure S13 (Supporting Information). The Stern–Volmer plot (Figure S14, Supporting Information)

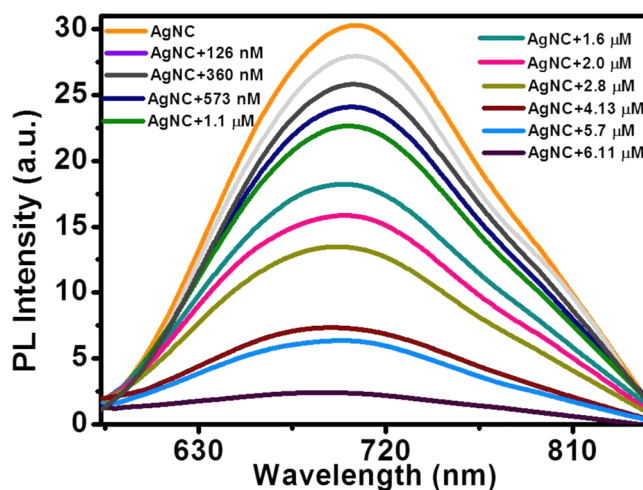


**Figure 9.** Fluorescence quenching of NC3 upon the gradual addition of  $\text{Hg}^{\text{II}}$  ions as indicated in the figure.

reveals the efficiency of quenching and the value of the Stern–Volmer constant for quenching of silver cluster fluorescence is estimated to be  $5.61 \times 10^5 \text{ M}^{-1}$ . UV–vis spectroscopic study is also used to examine the sensing of  $\text{Hg}^{\text{II}}$  ions by the red emitting silver cluster. The absorption band at 530 nm is gradually quenched after the gradual addition of  $\text{Hg}^{\text{II}}$  ions (Figure S15, Supporting Information). This absorption band is almost disappeared after the addition of 6.11  $\mu\text{M}$  of  $\text{Hg}^{\text{II}}$  ions into the cluster. The lower limit of detection of aqueous  $\text{Hg}^{\text{II}}$  ions sensing is 245 nM by using the UV–vis spectroscopic study. Time dependent UV–vis absorption and fluorescence emission spectral changes are shown in Figure S16 (Supporting Information) in the presence of  $\text{Hg}^{\text{II}}$  ions (3.7  $\mu\text{M}$ ). It is evident from Figure S16 (Supporting Information) that fluorescence quenching and absorption quenching occur with respect to the progress of time at 3.7  $\mu\text{M}$  concentration of  $\text{Hg}^{\text{II}}$  ions. Among the used metal ions for the sensing study, only  $\text{Cu}^{\text{II}}$  and  $\text{Pb}^{\text{II}}$  show very small quenching of fluorescence. However,  $\text{Hg}^{\text{II}}$  shows total quenching of fluorescence. The quenching of fluorescence intensity may occur due to the binding interaction of the carboxylate group with the free metal ions ( $\text{Hg}^{\text{II}}$ ) or the sulfur with the free metal ions ( $\text{Hg}^{\text{II}}$ ). If the quenching of fluorescence of red emitting silver quantum cluster occurs through the interaction with sulfur and/or carboxylate group, the above mentioned metal ions are expected to reduce the fluorescence of red emitting silver quantum cluster. However,  $\text{Zn}^{\text{II}}$  and  $\text{Cd}^{\text{II}}$  are totally silent about fluorescence quenching and very small quenching occurs for  $\text{Cu}^{\text{II}}$  and  $\text{Pb}^{\text{II}}$  (Figure S13, Supporting Information). These observations totally ruled out the possibility of fluorescence quenching due to the interaction with sulphur and/or carboxylate group with metal ions. Moreover, thiol is not free as it is attached with the silver quantum cluster. This conclusion has been supported by the FT-IR data shown in Figure S11 (Supporting Information) and mentioned in the FT-IR Study section. The involvement of nitrogen is nil. This is because the synthesis of silver cluster was carried out at pH 7.46. At this pH, most of these amino groups are protonated in glutathione to form  $-\text{NH}_3^{(+)}$  (ammonium ions) as the  $\text{pK}_a$  value of the amine part of glutathione is 9.49. This precludes the participation of the nitrogen atom present in the glutathione as a chelating agent as the lone pair of nitrogen is already being used to form the  $-\text{NH}_3^{(+)}$  (ammonium ions).<sup>51</sup> Thus, only free carboxylic

acid and thiol groups can engage in chelating silver for the stabilization of the silver cluster.<sup>52</sup> Thus, interaction between functional groups of glutathione (amine, carboxylic acid or thiol) and Hg<sup>II</sup> ions cannot explain the fluorescence quenching of the silver cluster. The explanation for the fluorescence quenching of the silver cluster in the presence of mercury ions lies somewhere else. This can be explained in light of metal–metal interactions. The metal center has a d<sup>10</sup> electronic configuration and it can participate in a strong interaction with the closed-shell d<sup>10</sup> electronic configuration of the other metal ion, as suggested by a previous theoretical calculation.<sup>53</sup> This d<sup>10</sup>–d<sup>10</sup> interaction is popularly known as metallophilic interaction.<sup>54</sup> In this study, the fluorescence quenching can be due to the strong 4d<sup>10</sup>–5d<sup>10</sup> metallophilic interaction between the silver quantum cluster and Hg<sup>II</sup> ions in water.<sup>55</sup> This leads to the aggregation of this cluster to a bigger size and this causes the quenching of fluorescence (Figure S17, Supporting Information). The very strong interaction of the silver quantum cluster with the Hg<sup>II</sup> ions can result in an enthalpy change after addition of the Hg<sup>II</sup> ions. The enthalpy obtained for the proposed interaction between the silver cluster and Hg<sup>II</sup> ions is high (2508 KJ mol<sup>-1</sup>). However, the enthalpy change is 5852 KJ mol<sup>-1</sup> due to the interaction between glutathione and Hg<sup>II</sup> ions and this is much higher than enthalpy change for silver cluster and Hg<sup>II</sup> ion interaction.<sup>56</sup> The higher value of the enthalpy change between the peptide and Hg<sup>II</sup> ions indicates a strong binding of glutathione with the Hg<sup>II</sup> ion. However, the enthalpy change for the interaction between the silver quantum cluster and Hg<sup>II</sup> ions is much less than that of the glutathione–Hg<sup>II</sup> system. This indicates the very good stabilization of the silver cluster by the bio-active peptide glutathione. The enthalpy change for the Ag cluster–Hg<sup>II</sup> interaction is almost half of the enthalpy change for the glutathione–Hg<sup>II</sup> complex, thus it can be mentioned that there is a possibility that Hg<sup>II</sup> forms a 1:2 complex with free glutathione, whereas only a 1:1 interacting species is possible for the formation of the glutathione–Ag cluster complex. The interaction between the silver nanomaterial and Hg<sup>II</sup> ions has also been considered previously by several research groups.<sup>57–59</sup> However, in this study, we have correlated the interaction between the silver quantum cluster and Hg<sup>II</sup> ions by using the measurement of thermodynamic properties (enthalpy change) during the process of interaction. The interaction between the peptide stabilized silver cluster with Hg<sup>II</sup> ions also causes a considerable amount of heat change and this is determined by isothermal titration calorimetry. This heat change experiment was repeated several times to check its reproducibility. Enthalpy change ( $\Delta H$ ) during this process is 2508 KJ mol<sup>-1</sup> (determined from the difference between the two inflection points) (Figure S18, Supporting Information).

## CONCLUSIONS

This study demonstrates the synthesis of three different sized new silver clusters exhibiting blue, green, and red emission in water at physiological pH using the same silver salt (AgNO<sub>3</sub>), the same reducing agent (NaBH<sub>4</sub>), the same stabilizing agent (glutathione reduced form), and the same solvent system. This procedure is easy to handle, economically viable, and it is without the involvement of any toxic agents. This is a wonderful example of tuning the fluorescence emission from blue to red through green just by either changing the temperature or by varying the concentration of silver salt used. MALDI-TOF MS analyses show three different cluster

sizes Ag<sub>5</sub> (blue), Ag<sub>8</sub> (green), and Ag<sub>13</sub> (red). Moreover, this red emitting fluorescent cluster exhibits highly selective and very sensitive detection of toxic Hg<sup>II</sup> ions in water.

## ASSOCIATED CONTENT

### Supporting Information

Detailed Instrumentation, UV–vis, Fluorescence, FT-IR, FEG-TEM, and ITC plots. This material is available free of charge via the Internet at <http://pubs.acs.org>.

## AUTHOR INFORMATION

### Corresponding Author

\*A. Banerjee. Fax: +91-33-2473-2805. Tel: +91-33-2473-4971. E-mail: [bcab@iacs.res.in](mailto:bcab@iacs.res.in).

### Notes

The authors declare no competing financial interest.

## ACKNOWLEDGMENTS

S.R. and A.B. thank CSIR, NEW Delhi, India for financial assistance. S.R. also thanks IACS for financial support.

## REFERENCES

- (1) Shiang, Y.-C.; Huang, C.-C.; Chen, W.-Y.; Chen, P.-C.; Chang, H.-T. *J. Mater. Chem.* **2012**, *22*, 12972–12982.
- (2) Diez, I.; Ras, R. H. A. *Nanoscale* **2011**, *3*, 1963–1970.
- (3) Shibu, E. S.; Radha, B.; Verma, P. K.; Bhyrappa, P.; Kulkarni, G. U.; Pal, S. K.; Pradeep, T. *ACS Appl. Mater. Interfaces* **2009**, *1*, 2199–2210.
- (4) Jin, R. *Nanoscale* **2010**, *2*, 343–362.
- (5) Díez, I.; Jiang, H.; Ras, R. H. A. *ChemPhysChem* **2010**, *11*, 3100–3104.
- (6) Roy, S.; Banerjee, A. *Soft Matter* **2011**, *7*, 5300–5308.
- (7) Anand, U.; Ghosh, S.; Mukherjee, S. *J. Phys. Chem. Lett.* **2012**, *3*, 3605–3609.
- (8) Roy, S.; Palui, G.; Banerjee, A. *Nanoscale* **2012**, *4*, 2734–2740.
- (9) Adhikari, B.; Banerjee, A. *Chem. Mater.* **2010**, *22*, 4364–4371.
- (10) George, A.; Shibu, E. S.; Maliyekkal, S. M.; Bootharaju, M. S.; Pradeep, T. *ACS Appl. Mater. Interfaces* **2012**, *4*, 639–644.
- (11) Xie, J.; Zheng, Y.; Ying, J. Y. *Chem. Commun.* **2010**, *46*, 961–963.
- (12) Guo, W.; Yuan, J.; Wang, E. *Chem. Commun.* **2009**, 3395–3397.
- (13) Shang, L.; Dong, S. *J. Mater. Chem.* **2008**, *18*, 4636–4640.
- (14) Qu, F.; Li, N. B.; Luo, H. Q. *Anal. Chem.* **2012**, *84*, 10373–10379.
- (15) Huang, Z.; Pu, F.; Lin, Y.; Ren, J.; Qu, X. *Chem. Commun.* **2011**, *47*, 3487–3489.
- (16) Tanaka, S.-I.; Miyazaki, J.; Tiwari, D. K.; Jin, T.; Inouye, Y. *Angew. Chem., Int. Ed.* **2011**, *50*, 431–435.
- (17) Li, J.; Zhong, X.; Cheng, F.; Zhang, J.-R.; Jiang, L.-P.; Zhu, J.-J. *Anal. Chem.* **2012**, *84*, 4140–4146.
- (18) Lin, C.-A. J.; Yang, T.-Y.; Lee, C.-H.; Huang, S. H.; Sperling, R. A.; Zanella, M.; Li, J. K.; Shen, J.-L.; Wang, H.-H.; Yeh, H.-I.; Parak, W. J.; Chang, W. H. *ACS Nano* **2009**, *3*, 395–401.
- (19) Yu, Y.; Chen, X.; Yao, Q.; Yu, Y.; Yan, N.; Xie, J. *Chem. Mater.* **2013**, *25*, 946–952.
- (20) Makarava, N.; Parfenov, A.; Baskakov, I. V. *Biophys. J.* **2005**, *89*, 572–580.
- (21) Yu, J.; Patel, S. A.; Dickson, R. M. *Angew. Chem., Int. Ed.* **2007**, *46*, 2028–2030.
- (22) Yu, J.; Choi, S.; Richards, C. I.; Antoku, Y.; Dickson, R. M. *Photochem. Photobiol.* **2008**, *84*, 1435–1439.
- (23) Choi, S.; Yu, J.; Patel, S. A.; Tzeng, Y.-L.; Dickson, R. M. *Photochem. Photobiol. Sci.* **2011**, *10*, 109–115.
- (24) Sharma, J.; Yeh, H.-C.; Yoo, H.; Werner, J. H.; Martinez, J. S. *Chem. Commun.* **2010**, *46*, 3280–3282.



- (25) Xavier, P. L.; Chaudhari, K.; Verma, P. K.; Pal, S. K.; Pradeep, T. *Nanoscale* **2010**, *2*, 2769–2776.
- (26) Chaudhari, K.; Xavier, P. L.; Pradeep, T. *ACS Nano* **2011**, *5*, 8816–8827.
- (27) Duan, H.; Nie, S. *J. Am. Chem. Soc.* **2007**, *129*, 2412–2413.
- (28) Liu, Y.; Tsunoyama, H.; Akita, T.; Tsukuda, T. *Chem. Commun.* **2010**, *46*, 550–552.
- (29) Negishi, Y.; Iwai, T.; Ide, M. *Chem. Commun.* **2010**, *46*, 4713–4715.
- (30) Oh, E.; Susumu, K.; Goswami, R.; Mattoussi, H. *Langmuir* **2010**, *26*, 7604–7613.
- (31) Linnert, T.; Mulvaney, P.; Henglein, A.; Weller, H. *J. Am. Chem. Soc.* **1990**, *112*, 4657–4664.
- (32) Zheng, J.; Dickson, R. M. *J. Am. Chem. Soc.* **2002**, *124*, 13982–13983.
- (33) Xu, H.; Suslick, K. S. *ACS Nano* **2010**, *4*, 3209–3214.
- (34) González, B. S.; Blanco, M. C.; López-Quintela, M. A. *Nanoscale* **2012**, *4*, 7632–7635.
- (35) Huang, X.; Li, B.; Li, L.; Zhang, H.; Majeed, I.; Hussain, I.; Tan, B. *J. Phys. Chem. C* **2012**, *116*, 448–455.
- (36) Mathew, A.; Sajanlal, P. R.; Pradeep, T. *J. Mater. Chem.* **2011**, *21*, 11205–11212.
- (37) Wu, Z.; Lanni, E.; Chen, W.; Bier, M. E.; Ly, D.; Jin, R. *J. Am. Chem. Soc.* **2009**, *131*, 16672–16674.
- (38) Guével, X. L.; Spies, C.; Daum, N.; Jung, G.; Schneider, M. *Nano Res.* **2012**, *5*, 379–387.
- (39) Yeh, H.-C.; Sharma, J.; Han, J. J.; Martinez, J. S.; Werner, J. H. *Nano Lett.* **2010**, *10*, 3106–3110.
- (40) Bootharaju, M. S.; Pradeep, T. *Langmuir* **2011**, *27*, 8134–8143.
- (41) Muhammed, M. A. H.; Aldeek, F.; Palui, G.; Trapiella-Alfonso, L.; Mattoussi, H. *ACS Nano* **2012**, *6*, 8950–8961.
- (42) Leelavathi, A.; Rao, T. U. B.; Pradeep, T. *Nanoscale Res. Lett.* **2011**, *6*:123, 1–9.
- (43) Diez, I.; Kanyuk, M. I.; Demchenko, A. P.; Walther, A.; Jiang, H.; Ikkala, O.; Ras, R. H. A. *Nanoscale* **2012**, *4*, 4434–4437.
- (44) Yuan, X.; Setyawati, M. I.; Tan, A. S.; Ong, C. N.; Leong, D. T.; Xie, J. *NPG Asia Mater.* **2013**, *5*, e39.
- (45) Kawasaki, H.; Hamaguchi, K.; Osaka, I.; Arakawa, R. *Adv. Funct. Mater.* **2011**, *21*, 3508–3515.
- (46) Lin, C.-A. J.; Lee, C.-H.; Hsieh, J.-T.; Wang, H.-H.; Li, J. K.; Shen, J.-L.; Chan, W.-H.; Yeh, H.-I.; Chang, W. H. *J. Med. Biol. Eng.* **2009**, *29*, 276–283.
- (47) Wang, T.; Hu, X.; Dong, S. *Chem. Commun.* **2008**, 4625–4627.
- (48) Henglein, A. *Chem. Phys. Lett.* **1989**, *154*, 473–476.
- (49) Yuan, X.; Tay, Y.; Dou, X.; Luo, Z.; Leong, D. T.; Xie, J. *Anal. Chem.* **2013**, *85*, 1913–1919.
- (50) Adhikari, B.; Banerjee, A. *Chem.—Eur. J.* **2010**, *16*, 13698–13705.
- (51) Das, T.; Mondal, S.; Datta, A. K.; Bera, B. K.; Karmakar, P.; Mallick, S.; Mandal, A.; Ghosh, A. K. *Int. J. Life Sci. Pharma Res.* **2012**, *2*, L-76–L-88.
- (52) Pattanayak, S.; Priyam, A.; Paik, P. *Dalton Trans.* **2013**, *42*, 10597–10607.
- (53) Pyykkö, P. *Angew. Chem., Int. Ed.* **2004**, *43*, 4412–4456.
- (54) Sculfort, S.; Braunstein, P. *Chem. Soc. Rev.* **2011**, *40*, 2741–2760.
- (55) Goswami, N.; Giri, A.; Kar, S.; Bootharaju, M. S.; John, R.; Xavier, P. L.; Pradeep, T.; Pal, S. K. *Small* **2012**, *8*, 3175–3184.
- (56) Mondal, S.; Ghosh, S.; Ghosh, D.; Saha, A. *J. Phys. Chem. C* **2012**, *116*, 9774–9782.
- (57) Katok, K. V.; Whitby, R. L. D.; Fukuda, T.; Maekawa, T.; Bezverkhy, I.; Mikhailovsky, S. V.; Cundy, A. B. *Angew. Chem., Int. Ed.* **2012**, *51*, 2632–2635.
- (58) Siddiqui, S. A.; Bouarissa, N.; Rasheed, T.; Al-Assiri, M. S. *Mater. Res. Bull.* **2013**, *48*, 995–1002.
- (59) Sun, L.; Zhang, A.; Su, S.; Wang, H.; Liu, J.; Xiang, J. *Chem. Phys. Lett.* **2011**, *517*, 227–233.